THz-Streaking with Dielectric-Lined Waveguides

Francois Lemery

Klaus Floettmann

July 7, 2017 at UBS workshop

based on IPAC 2017 contribution MOPAB052

Motivation

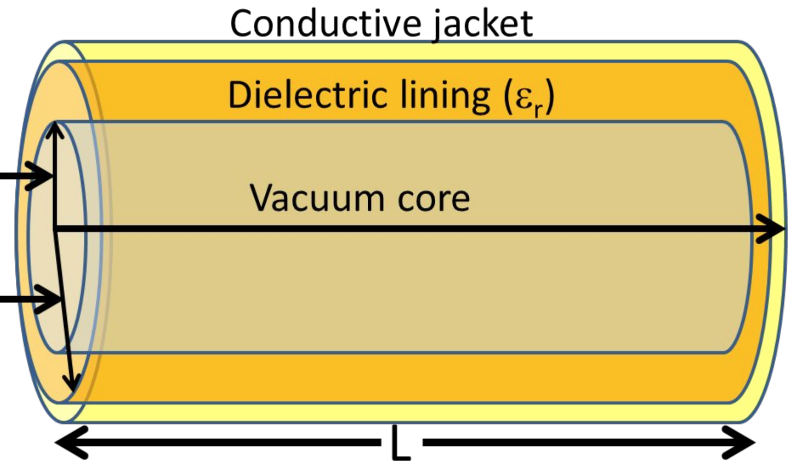

- Beam-driven acceleration in dielectric-lined waveguides (DLW) is a possible route toward efficient high-energy particle acceleration
- The DLW has a notorious beam breakup (BBU) problem; where the beam breaks apart from the dipole mode excitation.

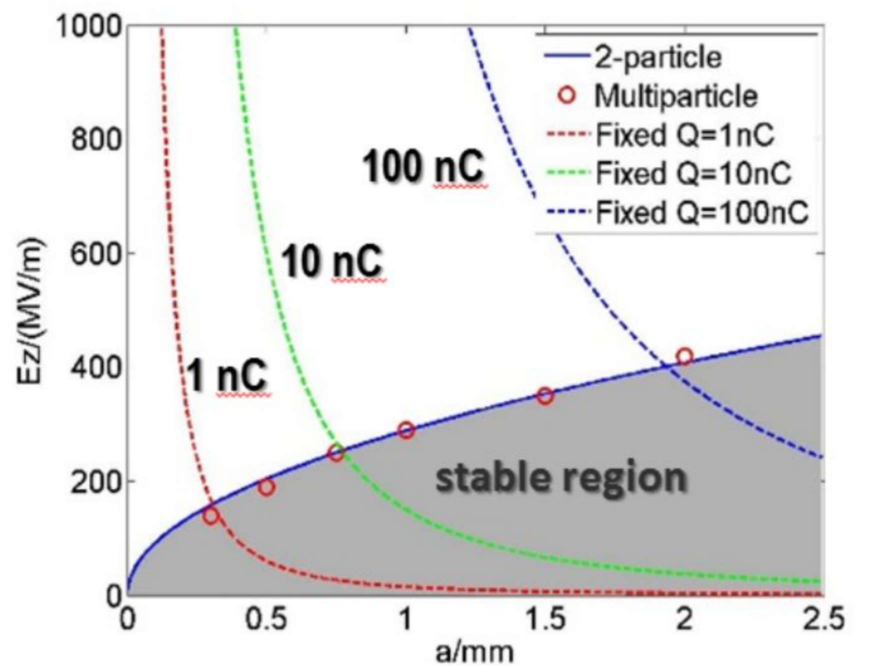

Beam breakup (BBU)
(C. Li et. al PhysRevSTAB.17.091302)

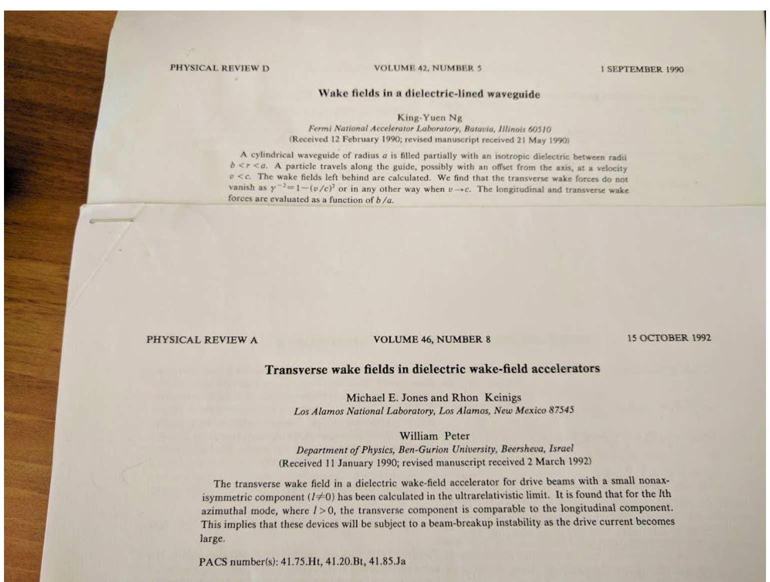

PHYSICAL REVIEW D VOLUME 42, NUMBER 5 1 SEPTEMBER 1990

Wake fields in a dielectric-lined waveguide

King-Yuen Ng
Fermi National Accelerator Laboratory, Batavia, Illinois 60510
(Received 12 February 1990; revised manuscript received 21 May 1990)

A cylindrical waveguide of radius a is filled partially with an isotropic dielectric between radii $b<r<a$. A particle travels along the guide, possibly with an offset from the axis, at a velocity $v<c$. The wake fields left behind are calculated. We find that the transverse wake forces do not vanish as $\gamma^{-2}=1-(v/c)^2$ or in any other way when $v\to c$. The longitudinal and transverse wake forces are evaluated as a function of b/a.

PHYSICAL REVIEW A VOLUME 46, NUMBER 8 15 OCTOBER 1992

Transverse wake fields in dielectric wake-field accelerators

Michael E. Jones and Rhon Keinigs
Los Alamos National Laboratory, Los Alamos, New Mexico 87545

William Peter
Department of Physics, Ben-Gurion University, Beersheva, Israel
(Received 11 January 1990; revised manuscript received 2 March 1992)

The transverse wake field in a dielectric wake-field accelerator for drive beams with a small nonaxisymmetric component ($l\neq 0$) has been calculated in the ultrarelativistic limit. It is found that for the lth azimuthal mode, where $l>0$, the transverse component is comparable to the longitudinal component. This implies that these devices will be subject to a beam-breakup instability as the drive current becomes large.

PACS number(s): 41.75.Ht, 41.20.Bt, 41.85.Ja

Schematic TDS setup

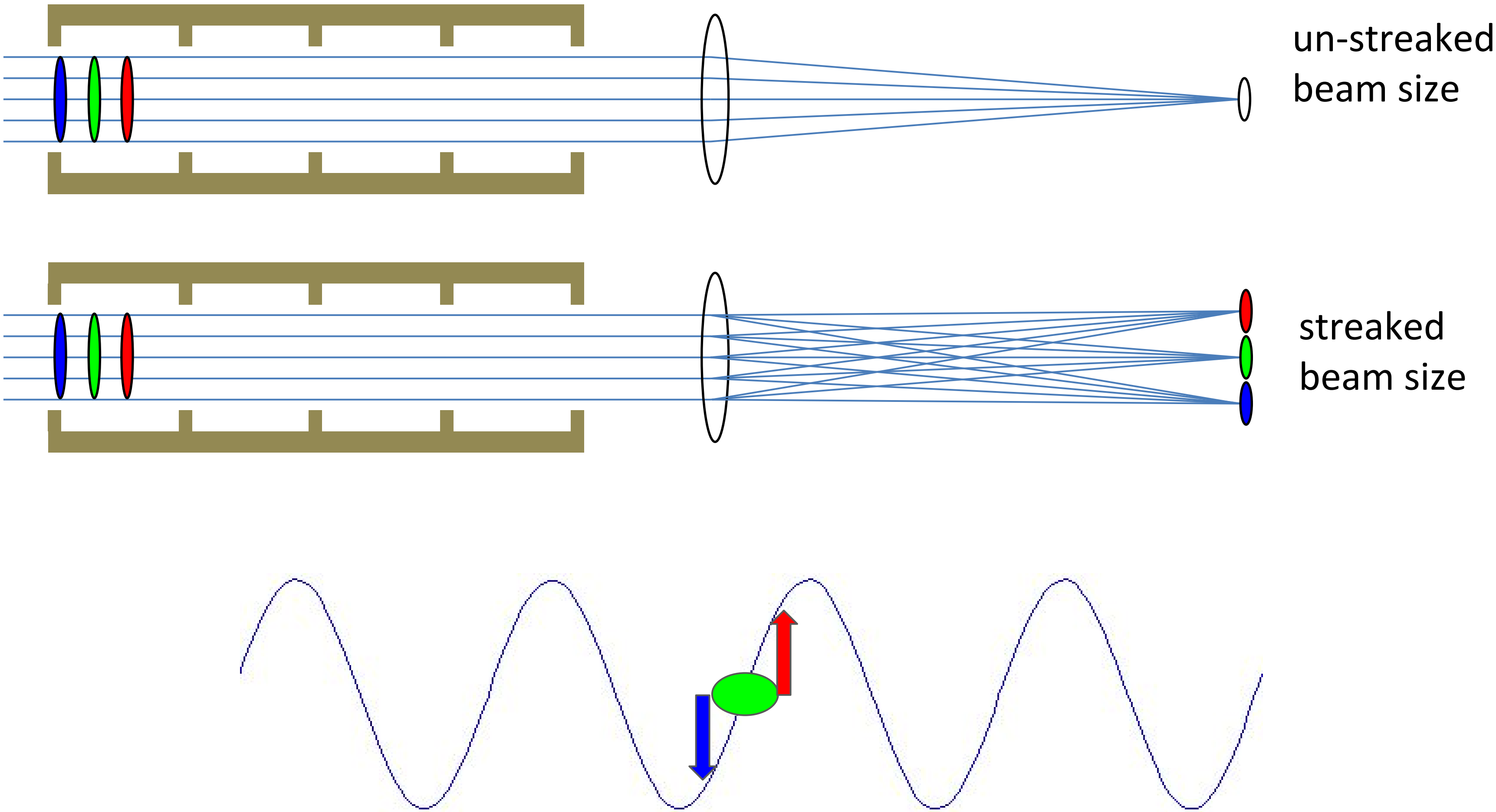

Resolution:

assume ideal optics with 90 degree phase advance between TDS and screen

$$R = \frac{\sigma_{sc,\text{ un-streaked}}}{\sigma_{sc,\text{ streaked}}} = \frac{\sigma'_{TDS,\text{ uncor.}}}{\sigma'_{TDS,\text{ introduced}}} = \frac{\varepsilon}{\sigma_y}\frac{cp_z}{ekV} = \frac{\varepsilon_n m_0 c^2}{\sigma_y ekV}$$

$$V = \int E_y(t,z) + c\beta_z B_x(t,z)dz$$

$$k = 2\pi/\lambda$$

a high resolution power $1/R$ requires:
- large integrated voltage V
- short wavelength, large k
- large beam size in the structure σ_y

Wavelength scaling of a TDS structure:

S-Band (3 GHz)

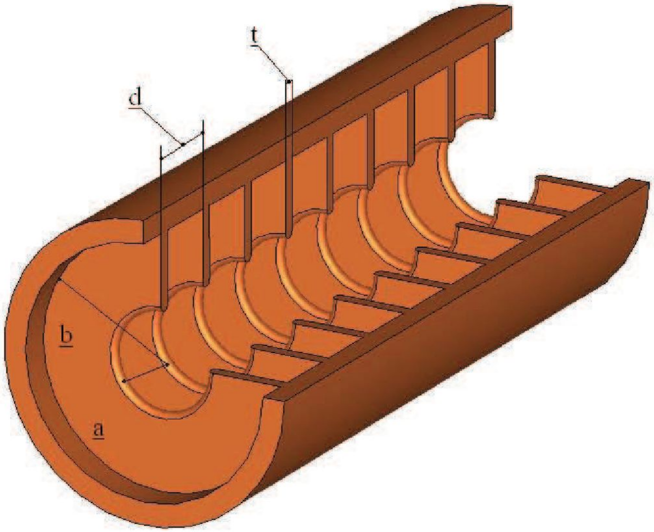

THz (300 GHz)

wavelength: λ = 10 cm λ = 1 mm

aperture radius: $a \approx 0.1\,\lambda$ = 1 cm $a \approx 0.1\,\lambda$ = 100 μm

beam size: $\sigma_y \approx (0.01\text{-}0.001)\,\lambda$ = 0.1-1 mm $\sigma_y \approx (0.01\text{-}0.001)\,\lambda$= 1-10 μm

$$k\sigma_y = \text{const.}$$

no profit if spot size is scaled with wavelength!

Mode description of transverse deflecting structures:

$$V = \int E_x(t,z) - c\beta B_y(t,z)dz = 0 \ldots 2\int E_x(t,z)dz$$

Panofsky-Wenzel theorem:

$V \neq 0$ only if $E_z(x) \neq 0$

but not only that:

- transverse deflecting fields have always 6 components
- the mode description can be done in terms of so-called hybrid modes HE+HM
- the HEM_{11} mode exists in iris loaded waveguides (small-pitch approximation) and in dielectric lined waveguides (fundamental mode)
- theory for all cases worked out in the 1960s and 70s, at that time for S-Band frequencies, e.g.

V. A. Vagin, V. I. Kotov,
Investigation of Hybrid Waves in a Circular Waveguide Partially Filled with Dielectric,
Soviet Physics - Technical Physics, Vol. 10, No. 7, (1966).

Dispersion Curve:

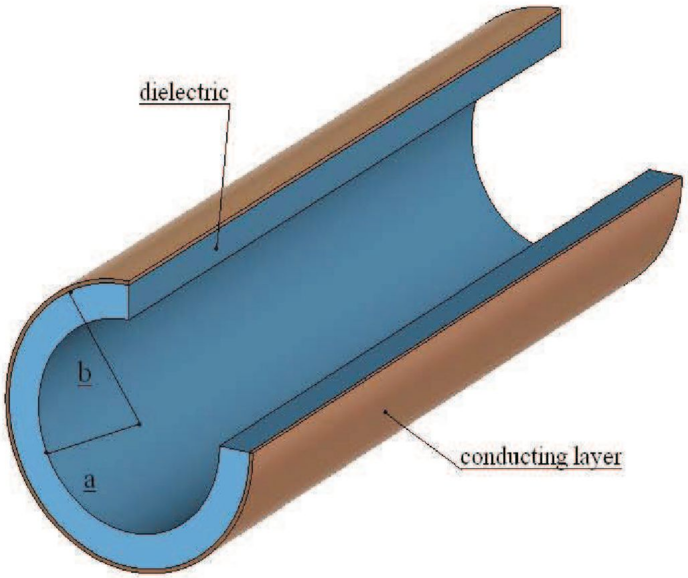

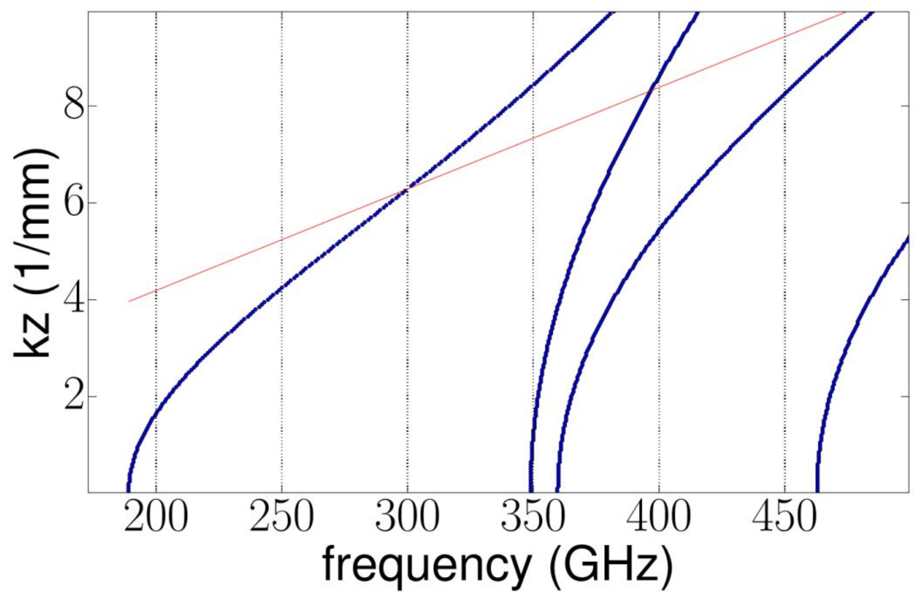

Dielectric lined waveguide: a = 0.3 mm, b = 0.398 mm, ε_r = 4.41 (Quartz) and dispersion curve. The 300 GHz structure is matched for v_p = 0.995c (5 MeV). The red line corresponds to the speed of light.

CST Results:

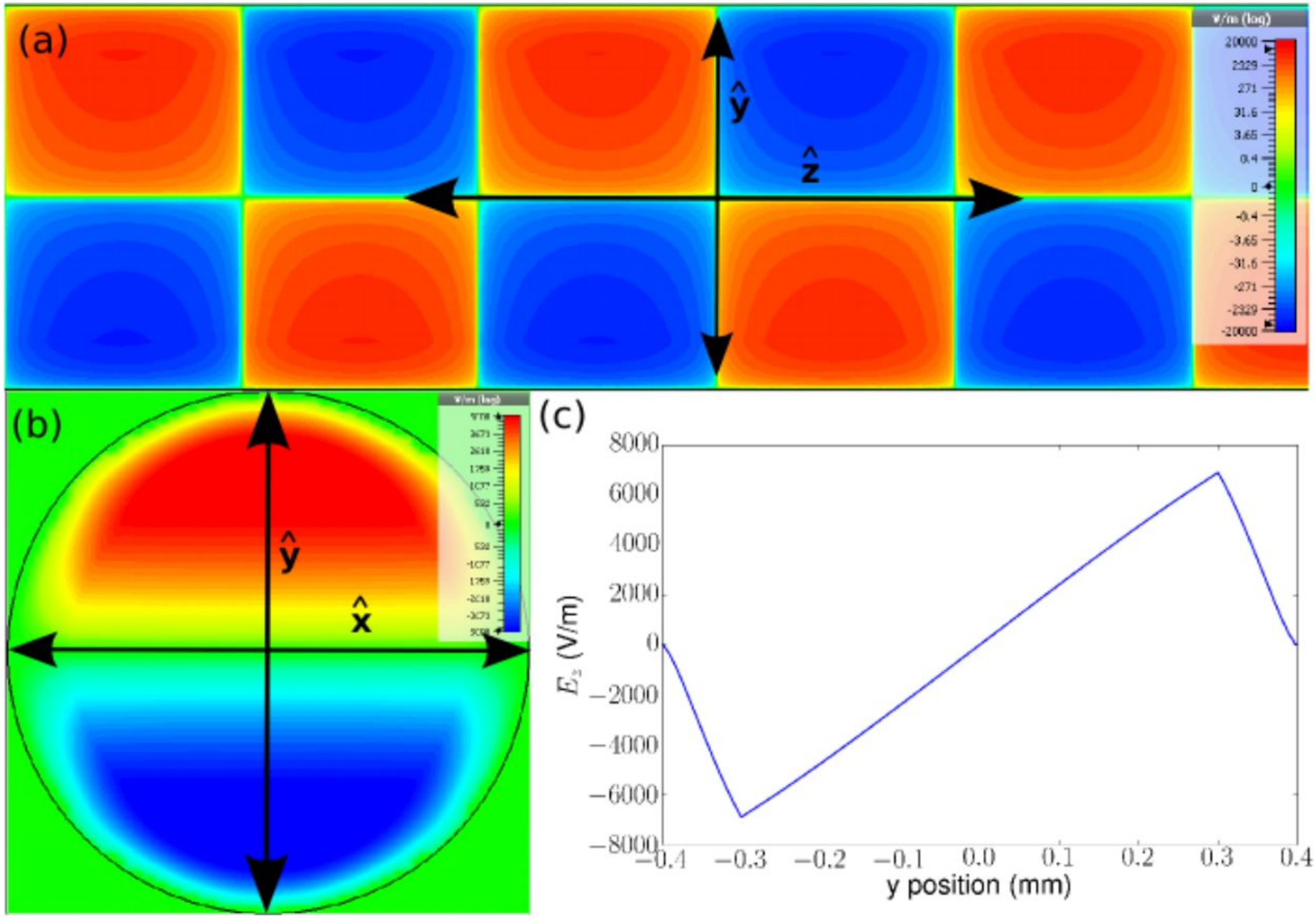

a) contour plot *y-z* in log scale
b) E_z vs. *x*, *y* at z = 1 cm in log scale
c) E_z vs. *y* at z = 1 cm

CST Results:

Panofsky-Wenzel theorem (or $\mathrm{rot}\,\vec{E} = \frac{\partial}{\partial t}\bar{B}$):

$$\frac{\partial}{\partial y} E_z \propto E_y + cB_x$$

a linear longitudinal field corresponds to a constant transverse force.

Confirmed with ASTRA simulation

$\sigma_y = 125\mu\mathrm{m}$, $R = 250\ \mu\mathrm{m}$

Comparison – REGAE case:

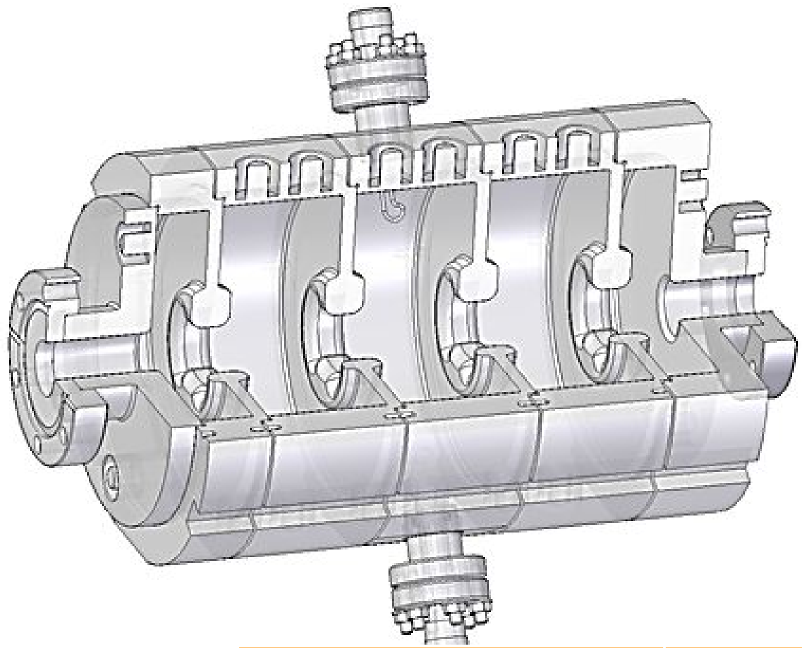

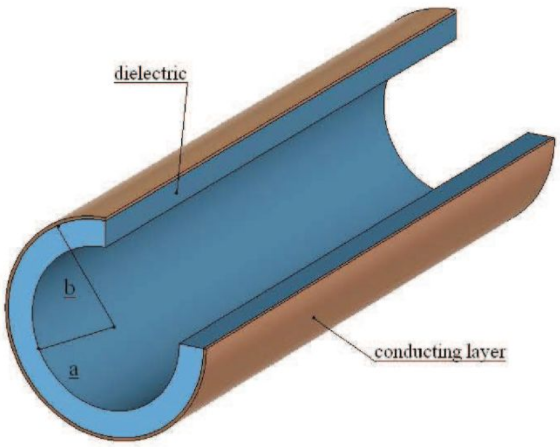

Type	S-band 20 cm	THz 3 cm
Power	5 kW	1.2 W
V	170 KV	9.2 kV
max. σ_y	0.4 mm	125 µm
$\sigma_y kV$	4.3 kV	7.2 kV
shunt imp.	36.7 MO/m	1.88 GO/m

Tunability

- We should expect high frequency devices to be sensitive.
- Can look to tune with frequency..
- Can also consider temperature tuning with some low-absorption plastics where heat expansion coef. 10^4. Some literature exists on treating HDPE for vacuum compatibility.

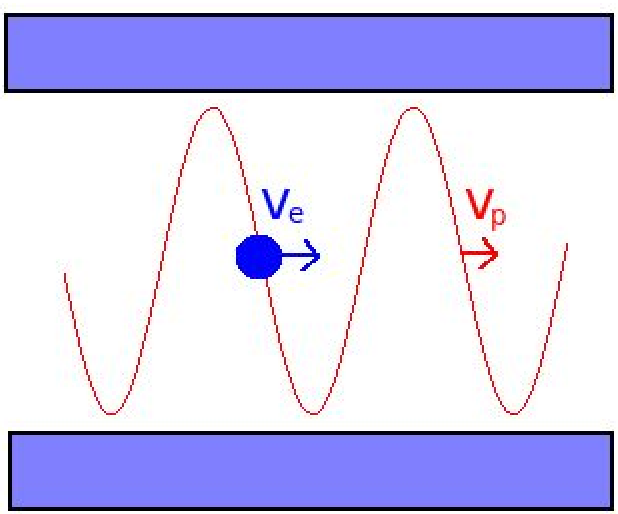

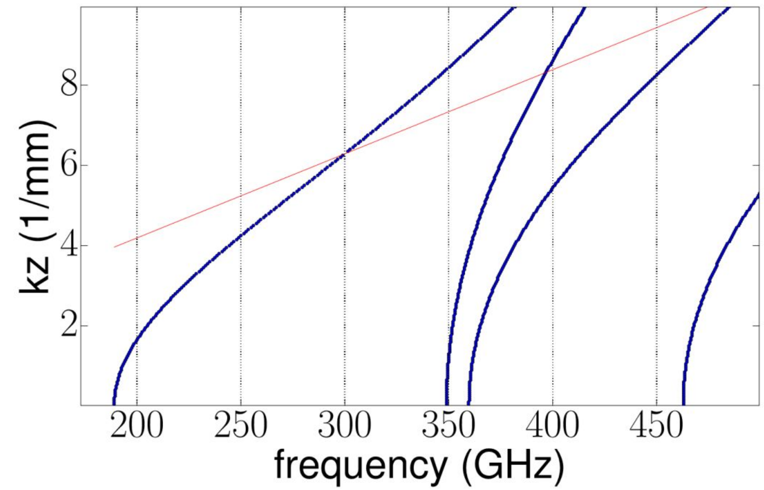

(28)

and let us consider the example from from Fig. 8, where $k_z^0 = \frac{\omega_0}{c} = \frac{2\pi 300GHz}{c}$, then,

$$k_z = \frac{\omega}{v_g} + \frac{\omega_0}{c}(1 - \frac{c}{v_g}), \tag{29}$$

introducing a dimensionless scaling factor $\omega = \alpha\omega_0$, simplifying and reorganizing leads to

$$k_z = \frac{\omega_0}{c}(n(\alpha - 1) + 1). \tag{30}$$

The phase velocity is given by

$$v_p = \frac{\omega}{k_z} = \frac{\alpha c}{n(\alpha - 1) + 1}, \tag{31}$$

finally, introducing the normalized phase velocity for simplicity $\beta_p = \frac{v_p}{c}$, we can solve for α in terms of β_p; after some algebra, the result is given by

$$\alpha = \frac{n - 1}{n - 1/\beta_p}. \tag{32}$$

As an example, a phase velocity change of 0.01c (e.g. from $v_p = c$ to $v_p = .99c$) can be achieved by a frequency change of $\alpha = 1.009$; i.e. a frequency shift from $f = 300\ GHz$ to $f = 302.7\ GHz$. We note smaller n generally has larger impact on v_p for a given frequency shift.

Control over the THz-generation frequency would be a valuable asset to control the accelerating conditions inside the structure.

THz waveguides beyond THz streaking:

- Dielectric lined hollow cylindrical metallic waveguides exhibit the lowest loss of all investigated waveguides at THz frequencies (1dB/m)
- Loss reduction in this waveguide is attributed to an ideal profile of the dominant hybrid HE mode.
- This mode profile also results in relatively low dispersion and very high coupling efficiency.

THz waveguides beyond THz streaking:

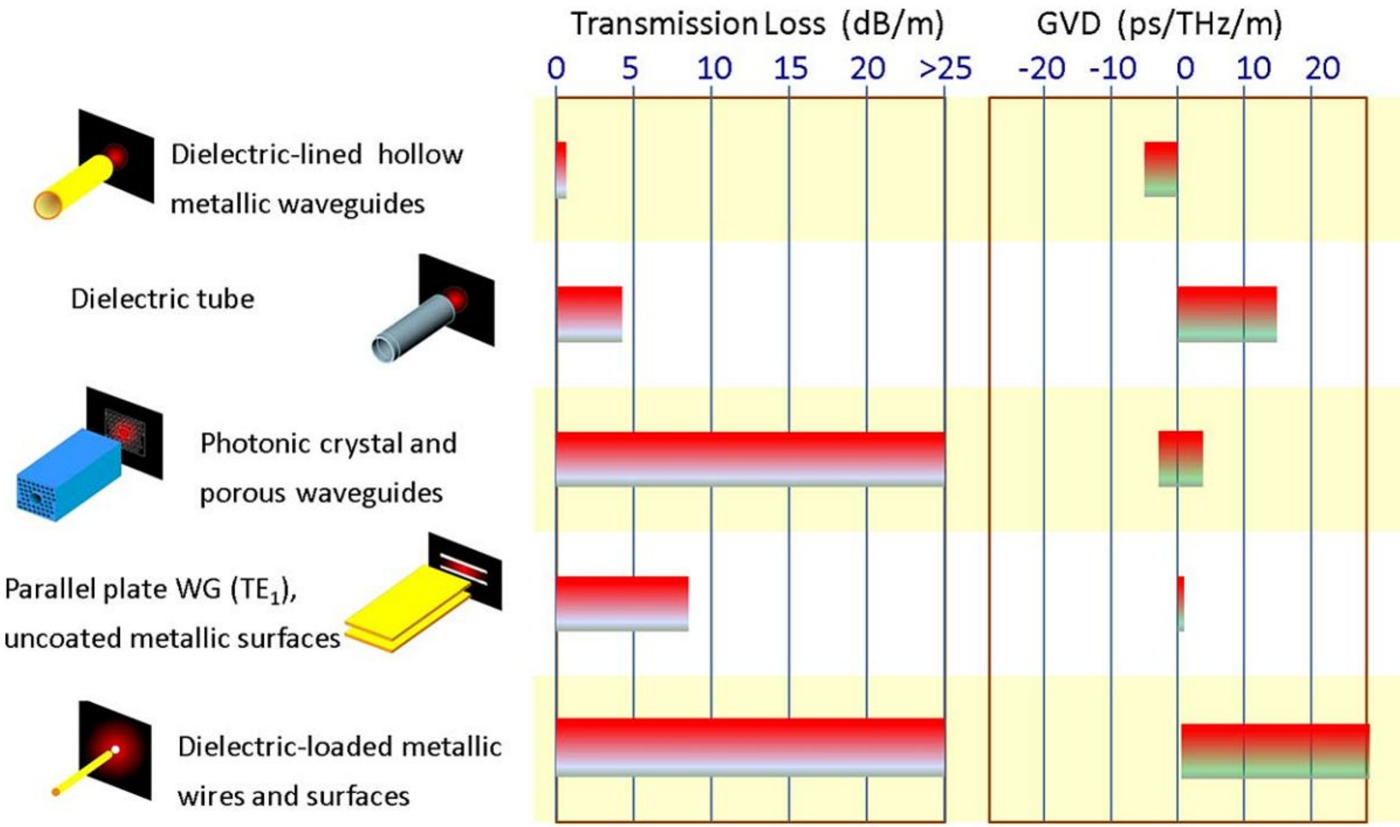

Common THz waveguides and their estimated transmission loss and dispersion characteristics in the region of 1–2 THz.

Oleg Mitrofanov et. al

Reducing Transmission Losses in Hollow THz Waveguides

IEEE Transactions on Terahertz Science and Technology, Vol. 1, No. 1, (2011).

THz waveguides – thick layer (~100 µm):

Proceedings of IPAC2017, Copenhagen, Denmark WEPAB122

EXPERIMENTAL DEMONSTRATION OF BALLISTIC BUNCHING WITH DIELECTRIC-LINED WAVEGUIDES AT PITZ

F. Lemery[1*], Dept. of Physics, University of Hamburg, 20355 Hamburg, Germany
P. Piot[2], Northern Illinois Center for Accelerator & Detector Development and Dept. of Physics, Northern Illinois University, DeKalb, IL 60115, USA
G. Amatuni[†], P. Boonpornprasert, Y. Chen, J. Good, B. Grigoryan[†], M. Krasilinikov, O. Lishilin, G. Loisch, S. Philipp, H. Qian, Y. Renier, F. Stephan,
Deutsches Elektronen-Synchrotron, 15738 Zeuthen, Germany
[1]also at the Center for Free-Electron Laser Science (CFEL), DESY, 22607 Hamburg, Germany
[2]also at Accelerator Physics Center, Fermi National Accelerator Laboratory, Batavia, IL 60510, USA

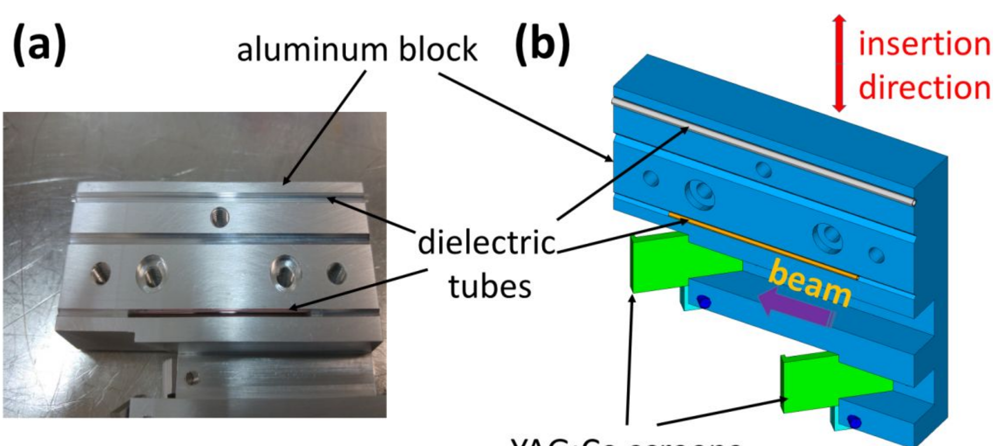

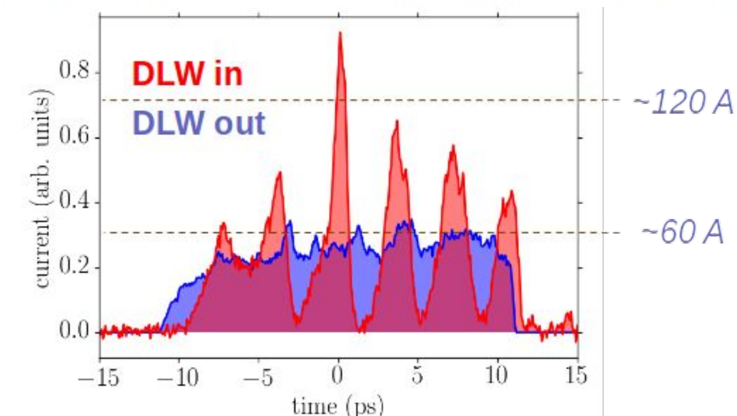

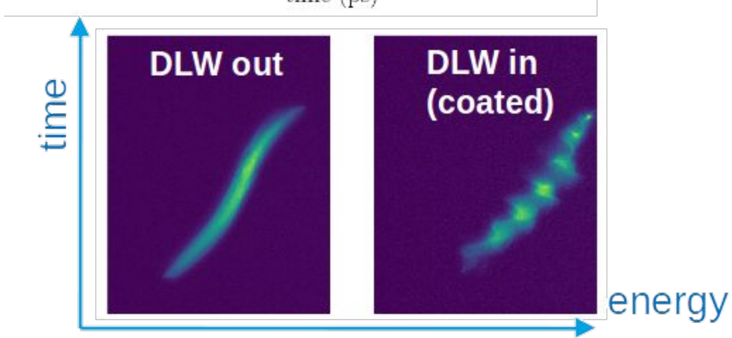

THz waveguides – thin layer (~10 μm):

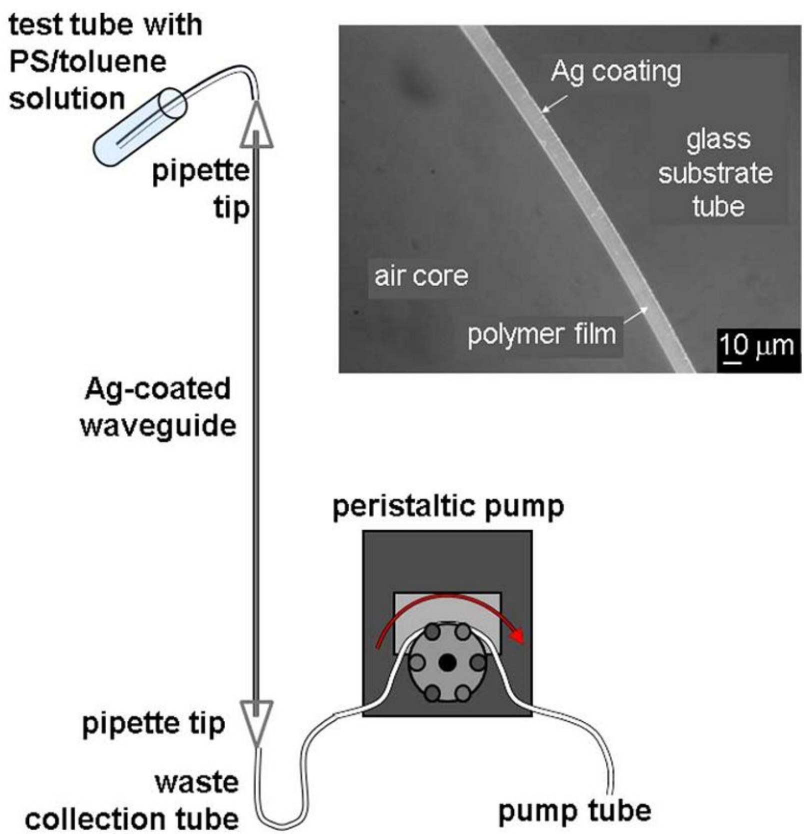

Apparatus to deposit polymer thin films over Ag films. Inset: an optical micrograph of a 2.2 mm bore diameter Ag/PS waveguide showing the PS layer.

Oleg Mitrofanv et al. ibid.

Acknowledgements

Thomas Vinatier

Ralph Assmann

Franz Kaertner

Flexible THz waveguides:

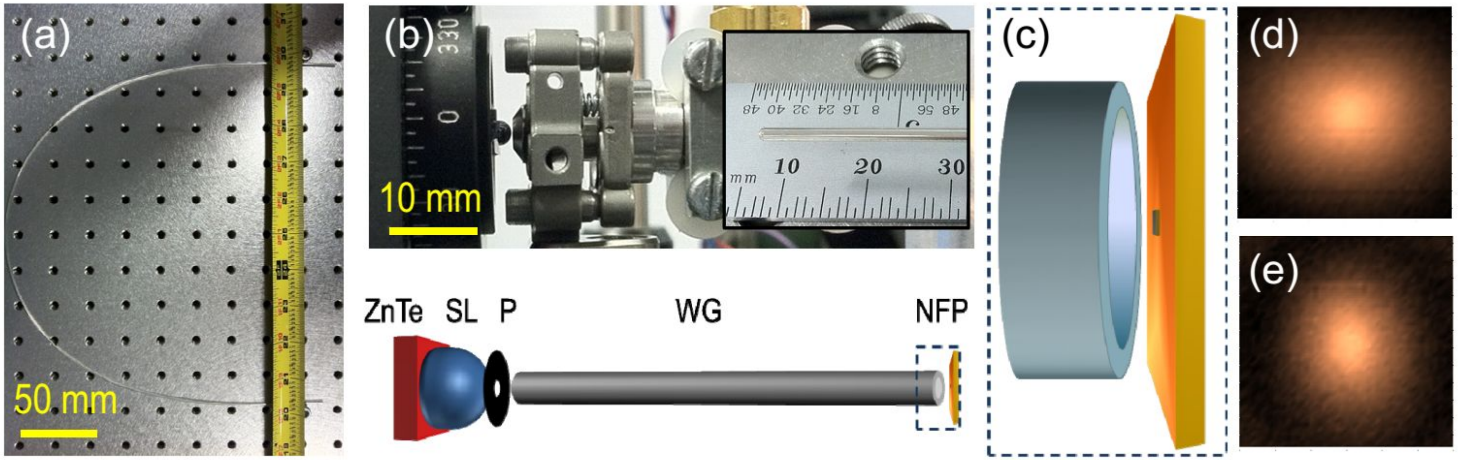

(a) Photograph of the PS-lined cylindrical metallic waveguide. (b) Photograph of the input section (top) and schematic of the near-field waveguide mode imaging system (bottom).
Inset: detail of the PS-lined cylindrical metallic waveguide. (c) Schematic of the subwavelength aperture near-field probe configuration. Near-field electric field Ex profiles (1.2 mm × 1.2 mm) at the output of the cylindrical metallic waveguide without (d) and with (e) the PS internal layer showing the TE11 and HE11 modes.

Oleg Mitrofanov et. al,
Terahertz wave transmission in flexible polystyrene-lined hollow metallic waveguides for the 2.5-5 THz band
Optics Express 21, 23748, (2013).

Backup – Near Field Probe:

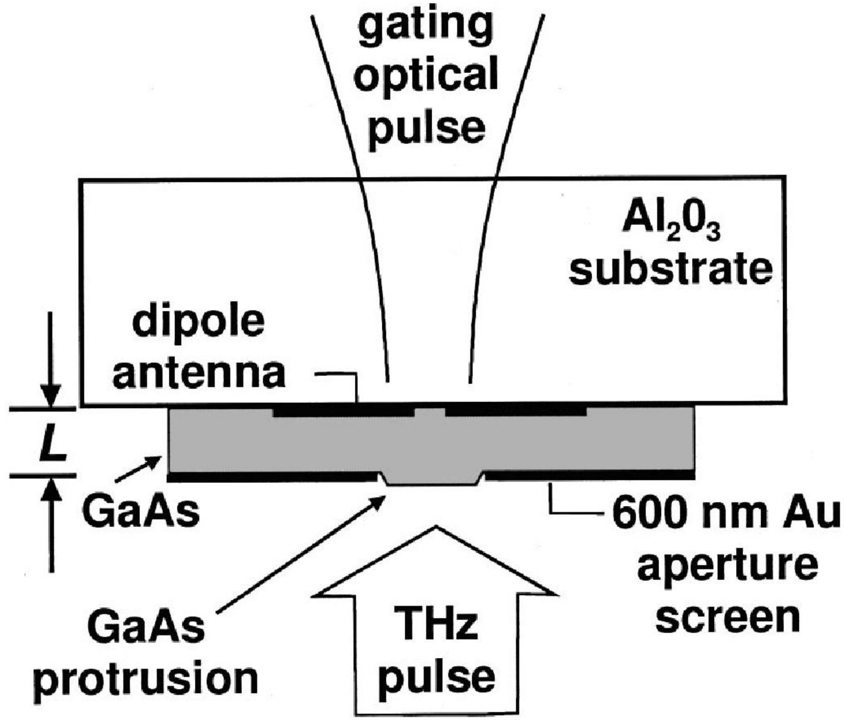

Schematic cross section of the near-field collection mode probe. L, thickness of the GaAs layer, sets the distance from the aperture to the dipole antenna.

Oleg Mitrofanov et. al,
Study of single-cycle pulse propagation inside a terahertz near-field probe
Appl. Phys. Lett Vol. 78, No. 2 (2001).

Backup – Mode structure:

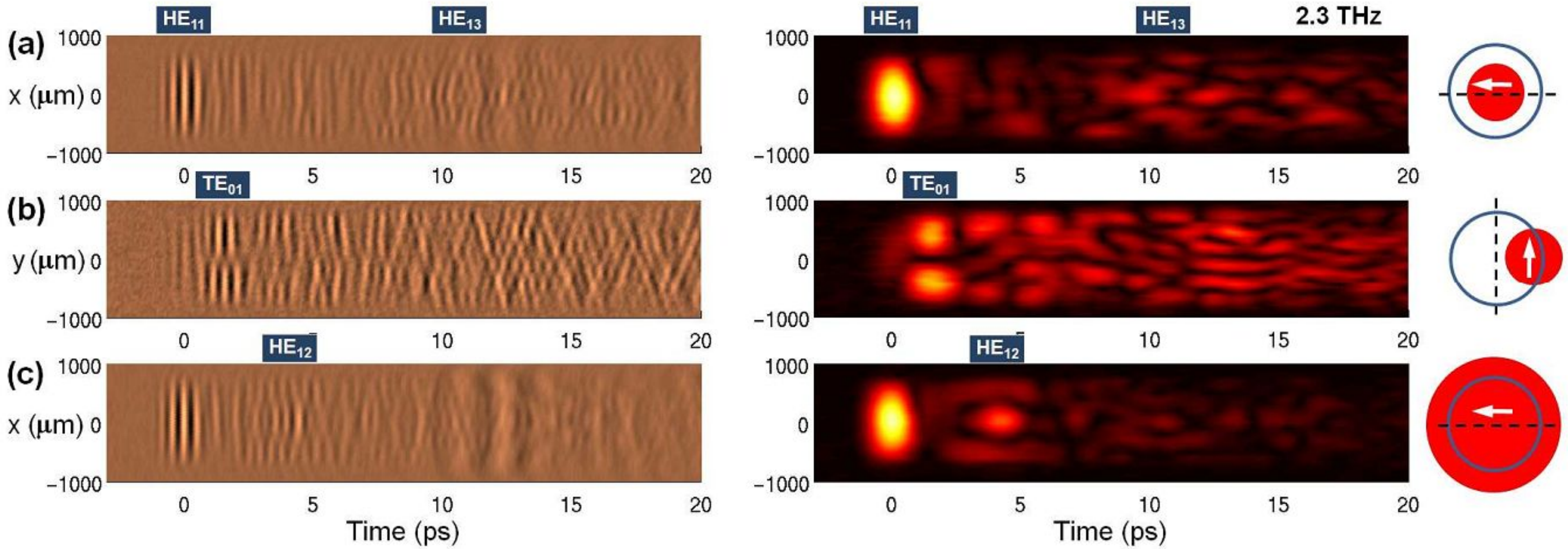

Space-time maps of the THz wave coupled to different combinations of waveguide modes. Maps of the electric field Ex(t) are shown in the left column and the corresponding maps of the field amplitude Ex(ω) at 2.3 THz are shown in the right column. The position of the input pinhole, the incident field polarization and the spatial scan lines are schematically shown
on the right.

Oleg Mitrofanov, James Harrington,
Dielectric-lined cylindrical metallic THz waveguides: mode structure and dispersion
Optics Express 18, 1898, (2010).